Animal Nutrition 18 (2024) 57–71

Contents lists available at ScienceDirect

Animal Nutrition

journal homepage: http://www.keaipublishing.com/en/journals/aninu/

Original Research Article

Dietary crude protein and protein solubility manipulation enhances intestinal nitrogen absorption and mitigates reactive nitrogen emissions through gut microbiota and metabolome reprogramming in sheep

Zhenbin Zhang [a, b, 1], Yiquan Sun [a, 1], Xinhuang Zhong [a], Jun Zhu [a], Sihan Yang [a], Yalan Gu [a, c], Xiang Yu [a], Yue Lu [a], Zhiqi Lu [a], Xuezhao Sun [d], Mengzhi Wang [a, b, *]

[a] *Laboratory of Metabolic Manipulation of Herbivorous Animal Nutrition, College of Animal Science and Technology, Yangzhou University, Yangzhou, 225009, China*
[b] *State Key Laboratory of Sheep Genetic Improvement and Healthy Production, Xinjiang Academy of Agricultural Reclamation Sciences, Shihezi, Xinjiang, 832000, China*
[c] *Shanghai Frontan Animal Health Co., Ltd., Shanghai, 201502, China*
[d] *AgResearch (Grasslands Research Centre), Palmerston North, 4410, New Zealand*

ARTICLE INFO

Article history:
Received 28 August 2023
Received in revised form
15 February 2024
Accepted 7 April 2024
Available online 12 April 2024

Keywords:
Soluble protein
Low-protein diet
Nitrogen metabolism
Reactive nitrogen
Fecal microbiota and metabolome
Energy and nitrogen utilization efficiency

ABSTRACT

Dietary nutrient manipulation (e.g. protein fractions) could lower the environmental footprints of ruminants, especially reactive nitrogen (N). This study investigated the impacts of dietary soluble protein (SP) levels with decreased crude protein (CP) on intestinal N absorption, hindgut N metabolism, fecal microbiota and metabolites, and their linkage with N metabolism phenotype. Thirty-two male Hu sheep, with an age of six months and an initial BW of 40.37 ± 1.18 kg, were randomly assigned to four dietary groups. The control diet (CON), aligning with NRC standards, maintained a CP content of 16.7% on a dry matter basis. Conversely, the experimental diets (LPA, LPB, and LPC) featured a 10% reduction in CP compared with CON, accompanied by SP adjustments to 21.2%, 25.9%, and 29.4% of CP, respectively. Our results showed that low-protein diets led to significant reductions in the concentrations of plasma creatinine, ammonia, urea N, and fecal total short-chain fatty acids (SCFA) ($P < 0.05$). Notably, LPB and LPC exhibited increased total SCFA and propionate concentrations compared with LPA ($P < 0.05$). The enrichment of the *Prevotella* genus in fecal microbiota associated with energy metabolism and amino acid (AA) biosynthesis pathways was evident with SP levels in low-protein diets of approximately 25% to 30%. Moreover, LPB and LPC diets demonstrated a decrease in fecal NH_4^+–N and NO_2^-–N contents as well as urease activity, compared with CON ($P < 0.05$). Concomitantly, reductions in fecal glutamic acid dehydrogenase gene (*gdh*), nitrite reductase gene (*nirS*), and nitric oxide reductase gene (*norB*) abundances were observed ($P < 0.05$), pointing towards a potential reduction in reactive N production at the source. Of significance, the up-regulation of mRNA abundance of AA and peptide transporters in the small intestine (duodenum, jejunum, and ileum) and the elevated concentration of plasma AA (e.g. arginine, methionine, aspartate, glutamate, etc.) underscored the enhancement of N absorption and N efficiency. In summary, a 10% reduction in CP, coupled with an SP level of approximately 25% to 30%, demonstrated the

* Corresponding author.
E-mail address: mzwang@yzu.edu.cn (M. Wang).
[1] These authors contributed to this work equally.
Peer review under responsibility of Chinese Association of Animal Science and Veterinary Medicine.

Production and Hosting by Elsevier on behalf of KeAi

https://doi.org/10.1016/j.aninu.2024.04.003

potential to curtail reactive N emissions through fecal *Prevotella* enrichment and improve intestinal energy and N utilization efficiency.

1. Introduction

According to the United Nations dataset (FAOSTAT, 2021), livestock feed production accounts for about two-thirds of the total crop-cultivated land in the world. This is coupled with the increasing demand for livestock-derived proteins, which may intensify the competition between food for humans and feed for livestock (Cheng et al., 2022). Ruminants have the ability to maximize the utilization of plant biomass that is not directly edible by humans. Approximately, 60% of their feed is composed of human-inedible cellulose, which contributes to food security and reduces the environmental impact of farming activities, such as straw incineration (Tilman and Clark, 2014). However, ruminants exhibit lower nitrogen (N) utilization efficiency compared with monogastric animals (Uwizeye et al., 2020). This results in relatively higher reactive N losses and greenhouse gas emissions. Therefore, the development of sustainable systems that prioritizes environmental protection, resource conservation, and high product quality has become an essential prerequisite for ruminant production.

The Hu sheep, with a farming history of over a thousand years, is a unique and precious white breed in China, characterized by its strong reproductive capacity, stress resistance, and fast growth and development (Geng et al., 2003; Yue, 1996). It has been reported that precision dietary interventions can improve N efficiency in ruminants and lower their environmental footprint of reactive N emissions by implementing low N diets or adjusting the proportions of dietary protein fractions (Tan et al., 2021; Wu et al., 2022). In our previous studies, we primarily focused on rumen N metabolism in sheep, employing both in vitro and in vivo experiments to identify optimal dietary soluble protein (SP) gradients. The in vitro results suggested that adjusting SP levels to 30% or 40% of CP could result in the altered bacterial and protozoal communities, in turn obtaining higher N efficiency (Zhang et al., 2022). On the other hand, in an in vivo study when sheep were fed a diet with decreased dietary N content, dietary SP levels of about 25% to 30% appeared to be a crucial variable for preventing excessive N emissions while optimizing animal performance. This approach resulted in heightened ruminal microbiota richness and *Prevotella* abundance, which promoted nutrient fermentation and increased related metabolites such as unsaturated fatty acids and vitamin B_6 in the rumen (Zhang et al., 2021).

However, studies focusing solely on rumen N metabolism are insufficient to provide comprehensive insights into the reduction of reactive N emission. Additionally, the significance of hindgut N metabolism, particularly in feces directly excreted into the environment, should not be overlooked (Harris et al., 2016). For instance, NH_3 and N_2O emissions from livestock manure account for 49% and 30% of total agricultural emissions, respectively, with over 15% of cattle feed N being discharged into sewers through manure (Bai et al., 2016; van der Weerden et al., 2020). Therefore, to develop effective strategies for reducing reactive N emissions while maintaining sheep production performance, it is crucial to investigate the hindgut N metabolism and its associated microbiota.

This study aims to investigate the impact of dietary N level reduction and SP regulation on nutrient metabolism, particularly reactive N, in sheep feces, based on our prior in vivo experiments. The main objectives were as follows: (1) to compare the effects of reduced dietary N levels and varying SP levels on intestinal N absorption and fecal N metabolism, and (2) to elucidate the potential mechanistic relationships among fecal microbiota, microbial-derived metabolites, and reactive N emissions through dietary SP regulation. We hypothesized that oscillating dietary SP levels, coupled with decreased CP, could enhance intestinal N absorption and mitigate reactive N emissions by reshaping fecal microbiota and metabolites in sheep.

2. Materials and methods

2.1. Animal management, feedstuffs, and experimental design

2.1.1. Animal ethics statements

All procedures conducted on animals in this experiment were approved by the Animal Welfare Committee of Yangzhou Veterinarians under the Ministry of Agriculture of China (Protocol No. Syxk (Su) 2019-0029).

2.1.2. Animal management and experimental treatments

Thirty-two healthy male Hu sheep, with an age of 6 months and an initial BW of 40.37 ± 1.18 kg, were randomly allocated into four dietary treatment groups ($n = 8$ per group) and individually housed in pens. The four treatments included one control diet and three treatment diets. The control diet (CON) was formulated according to the nutritional requirements outlined in the National Research Council standard (NRC, 2007) for sheep with a BW of 40 kg and an average daily gain of 200 to 250 g/d. The CP content of the CON diet was 16.7% of the dry matter (DM) basis.

The three treatment diets (LPA, LPB, and LPC) had a 10% lower CP content compared with the CON diet. The SP proportion in each of treatment diets was adjusted to 21.2% (LPA), 25.9% (LPB), and 29.4% (LPC) of CP. All four diets were isoenergetic, and the three treatment diets were isonitrogenous and met 90% of the CP standard requirements. The target SP levels were achieved mainly by adjusting the amount of various concentrates added. The analysis method of feed SP is reported in Section 2.1.3.

Sheep were fed twice a day (08:00 and 18:00) with the feeding level of the diets on a DM basis set to 3% of the BW of sheep on a DM basis. The diet comprised a 50:50 forage-to-concentrate ratio (DM basis), and clean water was available at any time during the feeding period. The experiment included a 1-week adaptation period and a 4-week experimental period. Data on DM intake and average daily gain have been previously reported (Zhang et al., 2021).

2.1.3. Chemical analyses of feedstuffs

Roughage used in this experiment was a mixed silage of cabbage waste and rice straw, with a 6:4 ratio of cabbage waste to straw. Additionally, 0.035 g/kg of *Lactobacillus plantarum* and 0.250 g/kg of cellulase were added to enhance fermentation. Concentrates, including corn, soybean meal, wheat bran, corn protein meal, and premix, were purchased from commercial feed suppliers.

The nutritional levels of the four diets were analyzed according to the standard methods of Association of Official Analytical Chemicals (AOAC, 2005). The DM content was determined by

drying triplicate samples at 105 °C to a constant weight. The CP content (N × 6.25) was analyzed using a Kjeldahl apparatus (Kjeltec 2300, FOSS Analytical AB, Hoganas, Sweden). The ether extract (EE) content was quantified using a Soxhlet extractor (FOSS Soxtec8000, Denmark). The ash content was determined as the residue after combustion at 550 °C in a muffle furnace (SX2-12-10, Rongfeng, Shanghai, China). Furthermore, neutral detergent fiber (NDF) and acid detergent fiber (ADF) were sequentially determined via filter bag technology (ANKOM 2000; Ancom Technology Corp., Fairport, NY, USA). Calcium (Ca) and phosphorus (P) were measured via the disodium ethylenediaminetetraacetate complexometric titration method and ammonium vanadate molybdate colorimetric method, respectively. The digestive energy (DE) was calculated based on their formula proportions by retrieving feed raw materials from the China Feed Database (https://www.chinafeeddata.org.cn/).

The detection method for dietary protein solubility referred to the buffer-soluble N protocols of a previous publication (Licitra et al., 1996). This method entails measuring the mass fraction of protein dissolved in the borate-phosphate buffer for 1 h at 39 °C. The ingredients and nutrition levels of the four diets are reported in Table S1.

2.2. Collection and measurements of fecal samples

2.2.1. Fecal sample collection

During the last three days of the experiment, six sheep were randomly taken from each group for feces collection at 4 h after morning feeding. Feces were collected rectally and pooled within each individual animal. A total of 100 g of the pooled feces were stored at −80 °C for further analysis of fermentation parameters, carbon (C) and N (including inorganic N) contents, as well as enzyme activity. Additionally, 5 g of feces collected on the last day were snap-frozen in liquid N for subsequent DNA extraction and metabolomic analysis.

2.2.2. Determination of fecal pH, microbial protein (MCP), and contents of short-chain fatty acids (SCFA)

Fresh feces were homogenized with distilled water at a 1:5 ratio (w/v) to determine pH value and MCP content. The pH was determined immediately after homogenization using a pH meter (pHS-3C, Shanghai, China), while the MCP content was determined using the trichloroacetic acid precipitation method as described by Koontz (2014). Moreover, 1 g of feces sample was homogenized in 1 mL of metaphosphoric acid (25%, w/v) and 10 mL of phosphate-buffered saline (pH = 7.4). The homogenized feces were then centrifuged (12,000 × *g*, 10 min, 4 °C) to collect supernatant. The supernatant was filtered through a 0.22-μm membrane and analyzed for SCFA using a gas chromatograph (GC-14B, Shimadzu, Kyoto, Japan) according to the protocol described in our previous publication (Zhang et al., 2021).

2.2.3. Detection of fecal C, N, and inorganic N contents

The fecal total N (TN) content was analyzed using the Kjeldahl method as described in Section 2.1.3 and C content was measured using an elemental analyzer (RapidCS cube C Version, Elementar Analysensysteme GmbH, Germany). The C/N ratio was calculated as the ratio of C content to TN content. To determine the content of inorganic N, including ammonia N (NH_4^+−N), nitrate N (NO_3^-−N), and nitrite N (NO_2^-−N), which were analyzed by Nessler's reagent spectrophotometry, the phenol disulfonic acid method, and N-(1-naphthyl)-ethylenediamine photometric method, respectively, as described by previous protocols (Noyes, 1919; Sabharwal, 1990; Yuen and Pollard, 1954).

2.2.4. Fecal enzyme activity assay

The activities of urease, nitrate reductase, and nitrite reductase in fecal samples were measured using an enzyme labeling instrument (SpectraMax M5/M5e, Molecular Devices, USA) and commercial reagent kits (Solarbio Technology Co., Ltd., Beijing, China).

2.2.5. Fecal DNA extraction, 16S rRNA sequencing, and absolute quantification PCR

Fecal total genomic DNA was extracted using HiPure Soil DNA Kit (D3142B, Magen, Guangzhou, China) and the quality and quantity were measured using Nanodrop 2000 UV/Vis spectrophotometer (Thermo Fisher Scientific, Wilmington, DE, USA) before being stored at −80 °C. The 16S rRNA gene in the V3 to V4 hypervariable regions was amplified with the primers, 341F (5′-CCTACGGGNGGCWGCAG-3′) and 806R (5′-GGACTACHVGGGTW TCTAAT-3′), using the specific amplification reaction procedure referred to our previous report (Zhang et al., 2021). Sequencing was performed on the Illumina Novaseq PE250 platform (Genepioneer Biotechnologies Co., Ltd, Nanjing, China) according to the manufacturer's protocol to obtain paired-end (PE) reads. FLASH (version 1.2.11) was used to merge paired-end readings and fastp (version 0.20.0) was used to filter the quality of the original labels to obtain high-quality clean labels (Chen et al., 2018; Magoc and Salzberg, 2011). Then, chimeric sequences were detected and removed by Vsearch (version 2.15.0) to obtain valid labels (Rognes et al., 2016). Unique sequences with 97% similarity were clustered into representative operational taxonomic units (OTU) by applying Uparse (version 7.0.1001) (Edgar, 2013) and the taxonomic information was annotated following the Silva Database (http://www.arb-silva.de/) based on the Mothur algorithm (Chappidi et al., 2019). Finally, the sequence proportions in each classification level (phylum, class, order, family, and genus) were statistically analyzed based on the OTU abundance and annotation information.

The abundance of genes related to N transformation was quantified by absolute quantification PCR. Each target gene was cloned into the pMD19-T vector (TaKaRa Bio, China) and transformed into *Escherichia coli* DH5α competent cells. Then plasmid DNA was extracted using a plasmid extraction kit (TaKaRa Bio, China) and analyzed for DNA quality and its concentration was measured using a NanoDrop 2000 UV/Vis spectrophotometer. PCR reactions were performed in a 20-μL reaction mixture, including 10 μL SYBR real-time PCR premixture, 2 μL DNA template, 0.4 μL forward primer, 0.4 μL reverse primer, and 7.2 μL ddH_2O (Huang et al., 2015). Calibration curves (log DNA concentration versus an arbitrarily set cycle threshold value) for glutamic acid dehydrogenase gene (*gdh*), ammonia monooxygenase gene subunit A (*amoA*), nitrate reductase gene (*narG*), nitrite reductase gene (*nirS*/*nirK*), nitric oxide reductase gene (*norB*), and nitrous oxide reductase gene (*nosZ*) were constructed using serial dilutions of amplicons of single colonies. The gene copy number of the amplicon was calculated by multiplying the molar concentration of the amplicon and the Avogadro's constant. Each sample was performed in triplicate, and efficiencies of real-time PCR assays were over 95%, and R^2 was 0.99. Primers of the above target genes are reported in Table S2.

2.2.6. Liquid chromatography coupled with mass spectrometry (LC–MS/MS) metabolomics processing of feces samples and data analysis

Fecal samples (100 mg per sample) were ground with liquid N and the homogenate was resuspended with prechilled 80% methanol of 500 μL by vortexing. The samples were incubated on ice for 5 min and then centrifuged at 15,000 × *g* at 4 °C for 20 min. One milliliter of the supernatant was diluted to the final concentration containing 53% methanol by LC-MS/MS grade water. The samples

were subsequently transferred to a fresh Eppendorf tube and then centrifuged at 15,000 × *g* at 4 °C for 20 min. Finally, the supernatant was injected into the LC-MS/MS system.

LC-MS/MS analyses were performed using a Vanquish UHPLC system (Thermo Fisher, Germany) coupled with an Orbitrap Q Exactive HF-X mass spectrometer (Thermo Fisher, Germany) in Novogene Co., Ltd. (Beijing, China). Samples were injected into a Thermo Scientific Hypersil GOLD column (length 100 mm, internal diameter 2.1 mm, particle diameter 1.9 μm) using a 12-min linear gradient at a flow rate of 0.2 mL/min. The eluents for the positive polarity mode were eluent A (0.1% formic acid) and eluent B (methanol). The eluents for the negative polarity modes were eluent A (5 mmol/L ammonium acetate, pH 9.0) and eluent B (methanol). Q Exactive HF-X mass spectrometer was operated in positive/negative polarity mode with a spray voltage of 3.5 kV, a capillary temperature of 320 °C, a sheath gas flow rate of 35 psi, an aux gas flow rate of 10 L/min, an S-lens RF level of 60, and an aux gas heater temperature of 350 °C.

The raw data files generated by LC-MS/MS were preprocessed using Compound Discoverer 3.1 (CD3.1, Thermo Fisher, Germany) for peak alignment, peak picking, and quantitation of each metabolite. Subsequently, the peaks were matched against the mzCloud (https://www.mzcloud.org/), mzVault and MassList database to obtain accurate qualitative and relative quantitative results.

These metabolites were annotated using the KEGG database (Kanehisa and Goto, 2000) (https://www.genome.jp/kegg/pathway.html), HMDB database (Wishart et al., 2007) (https://hmdb.ca/metabolites), and LIPIDMaps database (Fahy et al., 2007) (http://www.lipidmaps.org/). Statistical analysis of metabolites and pathways was completed via the online platform MetaboAnalyst 5.0 (Pang et al., 2021) (accessed on 8th January 2023) (https://www.metaboanalyst.ca/MetaboAnalyst/faces/home.xhtml). This comprehensive approach allowed for a thorough examination of the metabolic profile and its associated pathways in our study.

2.3. Collection and measurement of blood and intestinal samples

2.3.1. Blood and intestinal collection

On the last day of the feeding period, sheep were fasted overnight and then after fasting with no access to water for 2 h, they were anesthetized by intravenous administration of sodium thiopental (0.125 mg/kg BW) with potassium chloride (10 mL). Blood samples (10 mL each animal) were collected through vacutainers containing ethylenediaminetetraacetic acid (EDTA). One part of each whole blood sample was used to separate the plasma by centrifugation at 3000 × *g* at 4 °C for 10 min. After removing the mesenteric lymph nodes and connective adipose tissue, tissue samples (1 to 2 cm in length and approximately 5 g each) were taken from each segment of the small intestines (i.e. duodenum, jejunum, and ileum) by thoroughly washing 3 times with pre-cooled phosphate buffered saline (PBS). The samples were then immediately frozen in liquid N and stored at −80 °C for further analysis.

2.3.2. Detection of blood biochemical indexes and analysis of plasma AA concentration

The whole blood samples were directly analyzed for common blood indicators, including white blood cells, red blood cells, hemoglobin, and platelets, using an automatic blood cell analyzer (BC-2600, Mindray, Shenzhen, China). The plasma concentrations of total protein, albumin, globulin, creatinine, ammonia, urea N, alkaline phosphatase, lactate dehydrogenase, cholesterol, triglycerides, high-density lipoprotein, and low-density lipoprotein in the plasma were determined using the commercial kits (Jiancheng Biotechnology Research Institute, Nanjing, China). The plasma AA concentration was measured using the external standard method with an AA automatic analyzer (Terrlink et al., 1994).

2.3.3. Isolation of RNA from intestinal samples and real-time PCR

The total RNA was extracted from small intestinal samples (duodenum, jejunum, or ileum) using the RNA simple Total RNA Isolation Kit in accordance with the manufacturer's instructions (TIANGEN Biotech, Beijing, China). The RNA concentration and integrity were determined using a NanoDrop 1000 UV/Vis spectrophotometer (Thermo Fisher Scientific, NY, USA) and an Agilent 2100 Bioanalyzer (Agilent Technologies, TX, USA). Samples for subsequent analysis had OD260/OD280 values ≥1.9 and RNA Integrity Number (RIN) ≥8.0. The first strand of cDNA was synthesized using the FastQuant RT Kit (TIANGEN Biotech, Beijing, China). The qRT-PCR was performed on the 7500 Real-Time PCR System (Applied Biosystems, CA, USA) and the reaction mixtures were preheated at 95 °C for 15 min, followed by 40 cycles of melting at 95 °C for 10 s and annealing at 60 °C for 32 s (Hu et al., 2020). Beta-actin and glyceraldehyde-3-phosphate dehydrogenase (*Gapdh*) served as reference genes. The relative gene expression was calculated using the $2^{-\Delta\Delta Ct}$ method and the mRNA abundance of target genes in CON was taken as the baseline for fold changes relative to treatments (Livak and Schmittgen, 2001). Primers of target genes of intestinal AA and peptide transporters are reported in Table S3.

2.4. Measurements of N absorption and N efficiency

During the last three days of the experimental period, feed intake was recorded for all sheep to determine N intake. Simultaneously, feces and urine were quantitatively collected using fecal and urine bags, respectively, and treated with H_2SO_4 (10%, v/v) to prevent N loss. Finally, 10% of the total amount of feces and urine was sampled for the quantification of fecal N excretion and urinary N excretion. The N content was determined using a Kjeldahl analyzer as described in Section 2.1.3. Nitrogen absorption was calculated as N intake minus N excretion and N efficiency was defined as N absorption/N intake.

2.5. Statistical analysis

All statistical analyses were performed using SPSS software (version 16.0, IBM Co. Ltd., NY, USA) (Norusis, 2008) and R program (version 3.6.1) (Chambers, 2008). The statistical model used was as follows: $Y_{ij} = \mu + T_i + S_j + \varepsilon_{ij}$, where Y_{ij} is the observation of dependent variables; μ is the overall mean; T_i is the fixed effect of treatment; S_j is the random sheep effect, and ε_{ij} is the residual error for the observation. The PROC GLM procedure and Tukey's method were used for multiple comparisons of blood biochemical indexes, fecal physicochemical indexes, and gene quantification. Significance was declared at $P < 0.05$, and a tendency was identified at $0.05 \leq P < 0.1$.

For the analysis and visualization of fecal microbiota and metabolome data, R packages including “UpSetR”, “vegan”, “ggplot2”, “tidyverse”, and “microbiomeViz” were utilized (Barnett et al., 2021; Conway et al., 2017; Oksanen et al., 2007; Wickham, 2011; Wickham et al., 2017). Fecal metabolites with variable importance in projection (VIP) > 1 and $P < 0.05$, as well as fold change (FC) ≥ 2 or FC ≤ 0.5, were considered to be differential metabolites. Volcano plots were employed to filter metabolites of interest based on $\log_2$(FC) and $-\log_{10}$(*P*-value) of metabolites using the “ggplot2” package (version 3.3.6). Clustering heatmaps were generated using the “Pheatmap” package with data normalized via z-scores of the intensity areas of differential metabolites. Spearman's rank correlations between fecal microbiota and microbial metabolites were analyzed and visualized using the “Psych”

(Revelle, 2017) and "ggcorrplot" packages, with the threshold of $|r| > 0.5$ and $P < 0.05$.

3. Results

3.1. Fecal fermentation indicators

Dietary treatments had no significant impact on pH value and MCP concentration ($P > 0.05$, Table 1), while all low-protein treatments (LPA, LPB and LPC) caused a decrease in the total SCFA concentration ($P < 0.05$) compared with the control. Notably, LPA had a lower concentration compared with LPB and LPC ($P < 0.05$). In addition, the proportion of propionate significantly decreased while the proportion of butyrate significantly increased in LPA compared with CON and LPC ($P < 0.05$). However, there was no difference in the percentage of acetate ($P > 0.05$) among the treatments.

With respect to branched-chained fatty acids, isobutyrate percentage was lower in LPA and LPB compared with CON and LPC ($P < 0.05$). However, no significant differences were found in valerate and isovalerate percentages among all groups ($P > 0.05$).

3.2. Different forms of N content, enzyme activity, and gene transcription levels related to N transformation in feces

The TN content in LPB was lower than CON ($P < 0.05$, Fig. 1A). However, no difference was observed in the C/N ratio among the treatments ($P > 0.05$, Fig. 1B). A decrease in inorganic N was found in LPB and LPC compared with CON ($P < 0.05$), specifically in NH_4^+–N content (Fig. 1C) and NO_2^-–N content (Fig. 1D). However, no difference was found in NO_3^-–N among the treatments ($P > 0.05$, Fig. 1E).

In terms of enzyme activity, urease activity was reduced by decreasing dietary protein or increasing the SP level ($P < 0.05$, Fig. 1F). LPB decreased nitrate reductase activity compared with CON ($P < 0.05$, Fig. 1G), while no difference was observed in nitrite reductase activity among the treatments ($P > 0.05$, Fig. 1H).

Regarding gene transcription levels (Fig. 1I), the abundance of the *gdh* gene was down-regulated in the three low-protein treatments (LPA, LPB and LPC) compared with CON with LPB being the lowest among these three treatments ($P < 0.05$). Additionally, LPB has a lower abundance of the *narG* gene compared with CON and LPA ($P < 0.05$), while no difference was observed between LPB and LPC ($P > 0.05$). Furthermore, LPB and LPC had decreased abundances of the *nirK* gene and the *norB* gene compared to CON ($P < 0.05$). No differences were found in *amoA*, *nirK*, and *nosZ* gene abundances among the treatments ($P > 0.05$).

Table 1
Fermentation and microbial metabolic products in the feces of sheep fed low-protein diets with different soluble protein (SP) levels.

Item	Treatments				SEM	*P*-value
	CON	LPA	LPB	LPC		
pH	6.81	6.82	6.79	6.77	0.021	0.652
MCP, mg/g digesta	13.62	12.92	13.82	11.50	0.670	0.531
Total SCFA, mmol/L	59.65^{a}	27.83^{c}	50.80^{b}	49.36^{b}	3.237	<0.001
Acetate, mol/100 mol	77.52	81.68	78.92	78.96	2.920	0.474
Propionate, mol/100 mol	12.58^{a}	4.85^{b}	10.28^{a}	11.10^{a}	0.785	<0.001
Butyrate, mol/100 mol	2.87^{b}	6.38^{a}	4.63^{ab}	2.84^{b}	0.522	0.002
Isobutyrate, mol/100 mol	3.90^{a}	1.85^{b}	1.63^{b}	4.04^{a}	0.356	0.007
Valerate, mol/100 mol	2.29	2.80	2.83	2.17	0.282	0.562
Isovalerate, mol/100 mol	0.84	1.04	0.92	0.89	0.110	0.807

MCP = microbial crude protein; SCFA = short-chain fatty acids; SEM = standard error of the mean.
$^{a-c}$Within a row, means without a common superscript differed at $P < 0.05$.
Treatments included CON (16.7% crude protein [CP] based on nutritional requirements), LPA, LPB, and LPC (CP decreased by approximately 10%, with SP proportions of 21.2%, 25.9%, and 29.4% of CP, respectively).

3.3. Fecal microbial diversity and taxonomic differences

The OTU numbers shared by the four treatments were 1252, which accounted for 58.5% of the total OTU number (Fig. 2A). The OTU numbers shared by LPB and LPC were the highest (105, 4.9%), and the specific OTU numbers for CON, LPA, LPB, and LPC were 42, 42, 72, and 120 (5.6%, highest), respectively. Fig. S1 indicated that low-protein treatments increased the species richness ($P < 0.05$; ACE and Chao1) while sample diversity (Shannon and Simpson) showed no significance among treatments. Beta-diversity results (PCoA based on Bray–Curtis dissimilarity matrix, Fig. 2B) revealed significant differences in the bacterial communities (PERMANOVA: $P = 0.009$).

In terms of taxonomic classification, Firmicutes (57.1% to 76.8%), Bacteroidetes (12.4% to 23.1%) and Proteobacteria (3.0% to 4.3%) were the top-3 dominant phyla (Fig. 2C); Ruminococcaceae (25.4% to 43.8%) and Lachnospiraceae (9.4% to 16.7%) were the dominant families (Fig. 2D), with *Ruminococcaceae UCG–005* (10.5% to 17.7%) and *Christensenellaceae R–7 group* (8.5% to 16.6%) accounting for the top-2 abundance at the genus level (Fig. 2E).

Significant taxonomic differences in bacterial classification among the four treatments were further analyzed (Fig. 2F, G; Table S4). *Psychrobacter* was enriched in CON with the highest linear discriminant analysis (LDA) score and had a higher abundance compared with the low-protein treatments ($P < 0.05$). Additionally, the abundance of *Prevotellaceae UCG-004* was also higher in CON than in LPB and LPC ($P < 0.05$; Table S4). Notably, Prevotellaceae (family), *Prevotella_1*, and *Prevotellaceae_UCG-001* were increased in LPB and LPC compared with CON and LPA ($P < 0.05$; Table S4) and enriched with an LDA score over 4. Furthermore, Muribaculaceae (family) and *Desulfovibrio* (LDA score > 3.5) were enriched in LPA and the abundance of *Desulfovibrio* in LPA was highest among all the treatments ($P < 0.05$). In addition, Patescibacteria (phylum), *Candidatus_Saccharimonas*, *Ruminiclostridium 9*, and *Lachnospiraceae UCG-004* were enriched in LPC (LDA score > 2.5), and the abundances of Patescibacteria, *Ruminiclostridium 9*, and *Lachnospiraceae UCG-004* were increased in LPB and LPC compared with LPA ($P < 0.05$; Table S4).

3.4. Fecal metabolome profile and pathway enrichment analysis

A total of 696 positive ion mode metabolites and 573 negative ion mode metabolites were identified from 24 fecal samples based on LC-MS/MS, projections to latent structures-discriminant analysis (PLS-DA) score plots and score results showed that the four treatments were clearly separated in different ion modes (Fig. S2A–F), with the corresponding R^2Y values ranging from 0.88 to 0.97, indicating the satisfactory effectiveness of the model. Subsequent principal component analysis (PCA) score plots showed the composition of positive (Fig. S3A) and negative (Fig. S3B) ion mode metabolites of different treatments, which mainly classified into metabolism (level 1). Except for global and overview maps (level 2), pathway "AA metabolism" was the highest both in positive and negative modes (Fig. S3C and D).

The volcano plots of differential metabolites compared in pairs showed differentially altered metabolites with VIP >1.0 and *q* (FDR-adjusted *P*-value) <0.05 (Fig. 3A). These metabolites were then classified into AA, peptides, and analogues (Fig. 3B), carbohydrates and carbohydrate conjugates (Fig. 3C), fatty acids and conjugates (Fig. 3D), and others (Fig. 3E). In addition, as the SP proportion increased in low-protein diets, the contents of amides (e.g. oleamide, stearamide, hexadecanamide, and oleoyl ethylamide) and AA (e.g. L-phenylalanine, DL-tryptophan, L-tyrosine, L-valine, and methionine) were found decreased in LPB and LPC compared with LPA (Fig. 3F, Table S5).

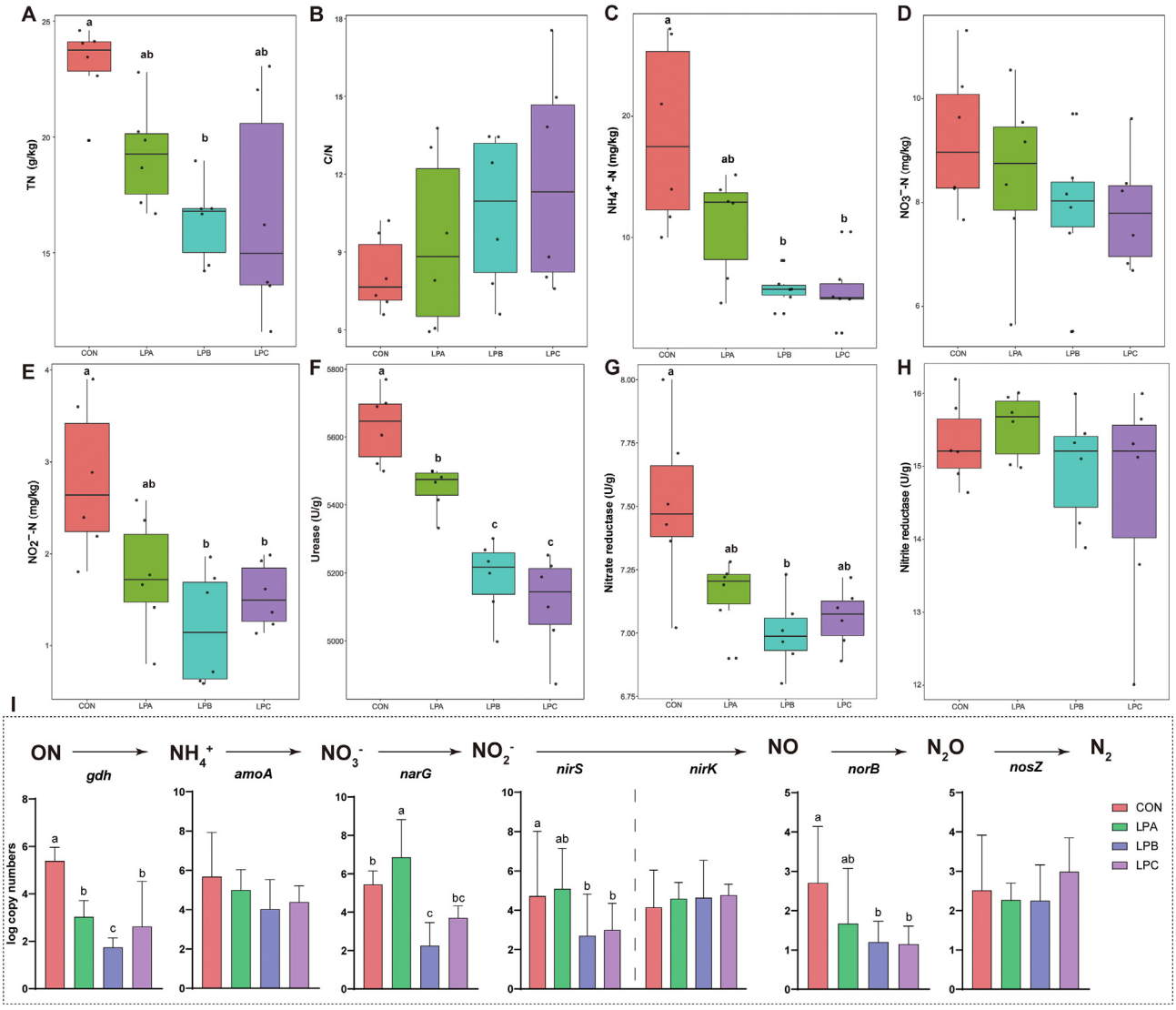

Fig. 1. Total nitrogen (TN) (A), carbon-to-nitrogen (C/N) ratio (B), NH_4^+–N (C), NO_3^-–N (D), NO_2^-–N (E), enzyme activity (F–H) and gene expression (I) related to N transformation in feces of sheep fed low-protein diets with different soluble protein (SP) levels. [a, b, c]Bars with different letters indicate a significant difference at $P < 0.05$. ON = organic nitrogen; NH_4^+–N = ammonia nitrogen; NO_3^-–N = nitrate nitrogen; NO_2^-–N = nitrite nitrogen; NO = nitric oxide; N_2O = nitrous oxide; *gdh* = glutamic acid dehydrogenase gene; *amoA* = ammonia monooxygenase gene subunit A; *narG* = nitrate reductase gene; *nirS*/*nirK* = nitrite reductase gene; *norB* = nitric oxide reductase gene; *nosZ* = nitrous oxide reductase gene. Treatments included CON (16.7% crude protein [CP] based on nutritional requirements), LPA, LPB, and LPC (CP decreased by approximately 10% with SP proportions of 21.2%, 25.9%, and 29.4% of CP, respectively).

Pathway enrichment analysis (Fig. 4A) revealed that 24 metabolic pathways were altered with decreased CP (LPA, LPB, and LPC). It is worth noting that amino sugar and nucleotide sugar metabolism pathways (e.g. tyrosine metabolism pathway, lysine degradation pathway, histidine metabolism pathway, and phenylalanine metabolism pathway) and biosynthesis of unsaturated fatty acids pathways were enriched in CON. As the SP proportion increased in low-protein diets, “pyruvate metabolism pathway”, “propanoate metabolism pathway”, “thiamine metabolism pathway”, and “phenylalanine and tyrosine and tryptophan biosynthesis pathways” were significantly enhanced.

Spearman's rank correlations indicated the complex relationships between bacterial genera (top-20 in abundance) and differential metabolites in feces. *Psychrobacter* (mainly enriched in CON) showed negative correlations with AA, peptides, and analogs (Fig. 4B). *Prevotella 1* (enriched in LPB) also exhibited similar patterns, which also showed negative correlations with most carbohydrates and carbohydrate conjugates, fatty acids and conjugates, linoleic acids and derivatives, pyrimidines and pyrimidine derivatives, etc. (Fig. S4).

3.5. Blood routine examination and plasma biochemical indexes

As shown in Table 2, different treatments had no significant impact on blood routine indicators (contents of white blood cells, red blood cells, hemoglobin, and platelets; $P > 0.05$). In terms of plasma biochemical indicators, low-protein treatments (LPA, LPB, and LPC) decreased the concentrations of creatinine, ammonia, and urea N ($P < 0.05$), while no differences were found in other biochemical indicators among all treatments ($P > 0.05$).

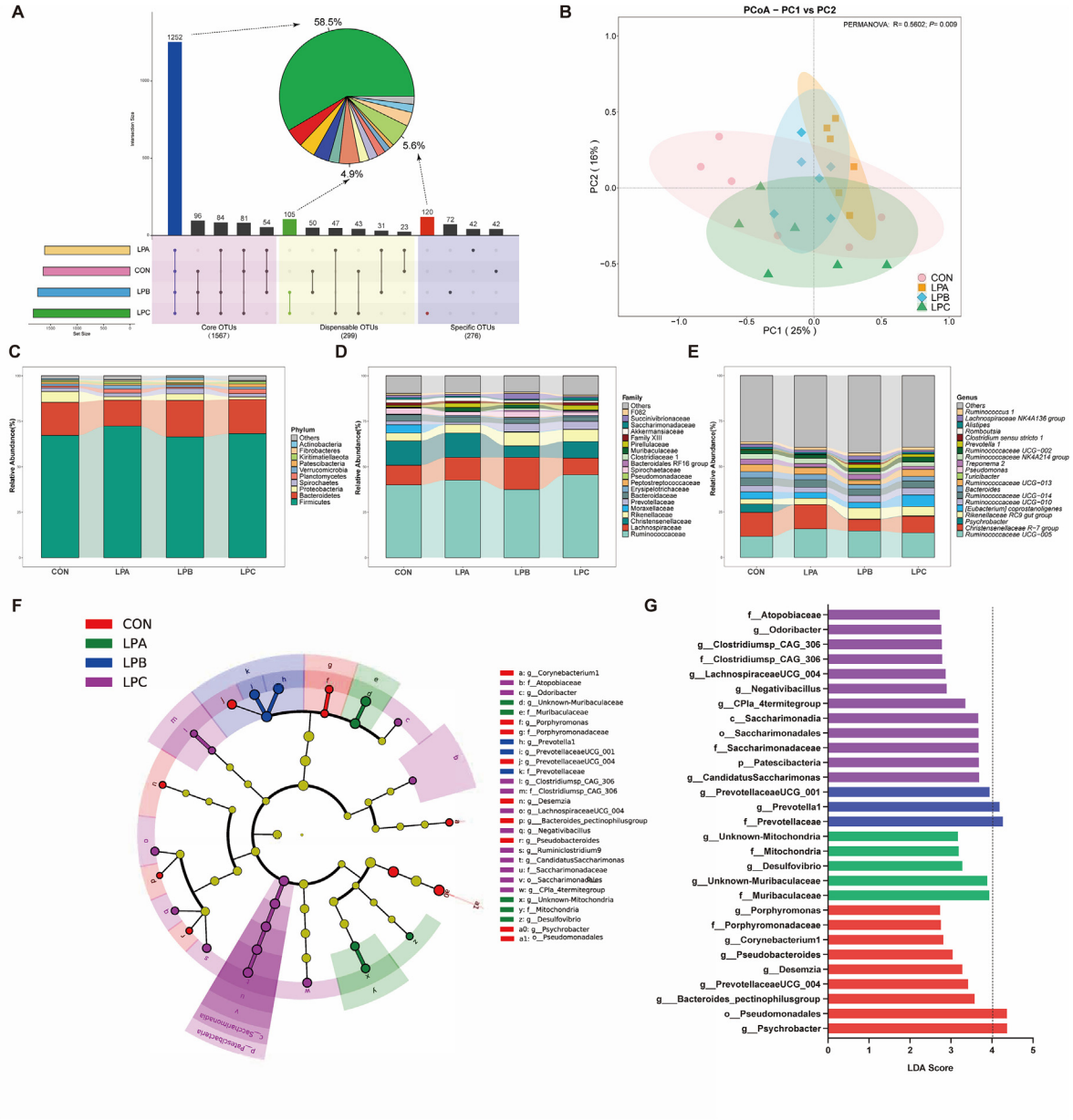

Fig. 2. Fecal microbiota composition and taxonomic differences of sheep fed low-protein diets with different soluble protein (SP) levels. (A) Histograms illustrating core operational taxonomic units (OTU) shared in three and four treatments, dispensable OTU present in two treatments, and specific OTU present in one treatment. (B) Principal coordinates analysis (PCoA) demonstrating the separation of microbial communities in feces among the four treatments based on the Bray–Curtis dissimilarity matrix. (C to E) Bacterial compositions in feces at the phylum (C), family (D), and genus (E) levels for CON, LPA, LPB, and LPC treatments. (F) Dendrogram indicating differentially enriched taxa in the rumen samples of four treatments, color-coded CON (red), LPA (green), LPB (blue), and LPC (purple). (G) Linear discriminant analysis (LDA) scores highlighting microbial OTU in the feces, with LDA score >2.5 marked. Treatments included CON (16.7% crude protein [CP] based on nutritional requirements), LPA, LPB, and LPC (CP decreased by approximately 10%, with SP proportions of 21.2%, 25.9%, and 29.4% of CP, respectively).

3.6. The mRNA abundance of intestinal AA/peptide transporters and plasma AA concentration

The mRNA expression analysis revealed that LPA treatment resulted in lower abundances of solute carrier family 1 member 1 (*SLC1A1*), solute carrier family 7 member 2 (*SLC7A2*), solute carrier family 7 member 8 (*SLC7A8*), and peptide/histidine transporter 1 (*PHT1*) in the duodenum, jejunum, and ileum compared with CON ($P < 0.05$, Fig. 5A). However, LPB and LPC treatment did not significantly differ from CON ($P > 0.05$). Additionally, in the duodenum, the mRNA abundance of *SLC1A5* was lower in LPA compared with CON ($P < 0.05$), while the mRNA abundance of *SLC7A1* was lower in LPA than in CON and LPB ($P < 0.05$). LPA treatment also decreased the mRNA abundance of *PepT1* ($P < 0.05$). The mRNA abundance of *PHT2* was lower in the three low-protein dietary treatments than the control diet ($P < 0.05$). Moreover, in the ileum, LPA treatment also resulted in a lower mRNA abundance of *PepT1* compared with CON ($P < 0.05$).

As shown in Fig. 5B, seven essential AA (EAA) and two non-essential AA (NEAA), including cysteine, histidine, lysine, phenylalanine, threonine, tryptophan, valine, alanine, and proline, were down-regulated in the low-protein treatments. It is worth mentioning that the concentrations of arginine, isoleucine, leucine, methionine, aspartate, glutamate, glutamine, citrulline, and ornithine were reshaped when the SP level was adjusted to 25.9% (LPB) or 29.4% (LPC) of CP in low-protein diets.

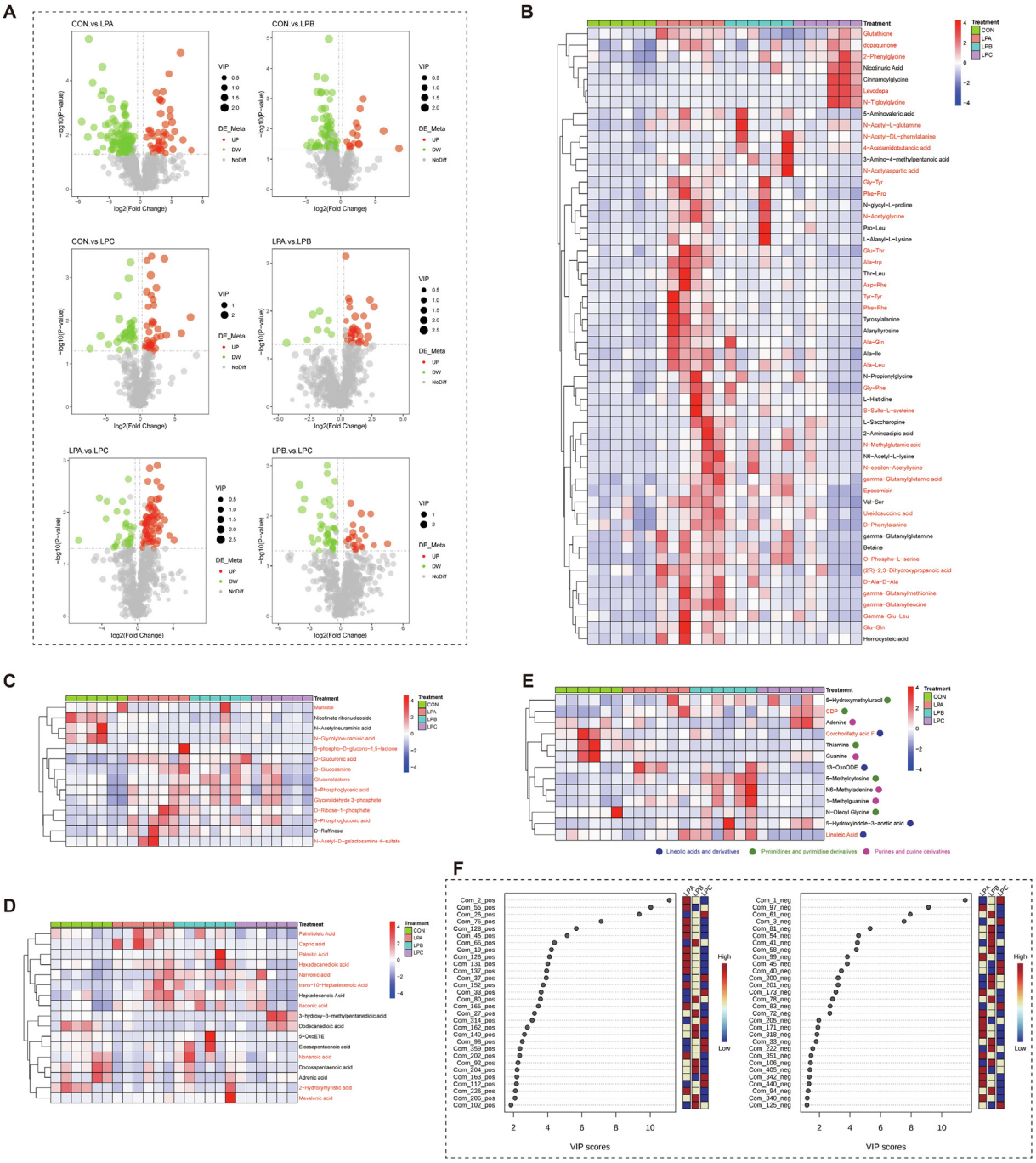

Fig. 3. Classification and summary of differential metabolites in the feces of sheep fed low-protein diets with different soluble protein (SP) levels. (A) Volcano plots illustrating differential metabolites comparisons (CON vs. LPA, CON vs. LPB, CON vs. LPC, LPA vs. LPB, LPA vs. LPC, and LPB vs. LPC). (B to E) Heatmaps presenting different metabolites among the four treatments, notably amino acids, peptides, and analogues (B), carbohydrates and carbohydrate conjugates (C), fatty acids and conjugates (D), and others (E). Black font indicating that metabolites were detected in positive mode, while red font indicating that those were detected in negative mode. (F) VIP scores highlighting key differential metabolites in the feces of sheep fed low-protein diets with different SP levels (LPA, LPB, and LPC) in positive/negative ion modes. Treatments included CON (16.7% crude protein [CP] based on nutritional requirements), LPA, LPB, and LPC (CP decreased by approximately 10%, with SP proportions of 21.2%, 25.9%, and 29.4% of CP, respectively).

3.7. N absorption and N efficiency

The data of N intake, N Excretion, N absorption, and N efficiency are detailed in Supplementary Table S6. In brief, dietary CP reduction led to a decrease in N intake ($P < 0.05$). Notably, N excretion decreased while N absorption and N efficiency increased ($P < 0.05$) when adjusting SP (% of CP) to 25.9 and 29.4, and specifically, N efficiency was improved by 12.2% and 8.5%, respectively, compared with CON.

3.8. Correlations of fecal microbiota, derived metabolites, and N metabolism phenotypes

Redundancy analysis (RDA) revealed that the C/N ratio was the primary factor affecting the fecal microbial community, followed by NH_4^+–N and NO_2^-–N (Fig. 6A). Notably, several bacterial taxa positively correlated with the C/N ratio, including OTU 892, 852, 1046, 348, 861, 1315, and 910, which mainly belonged to the

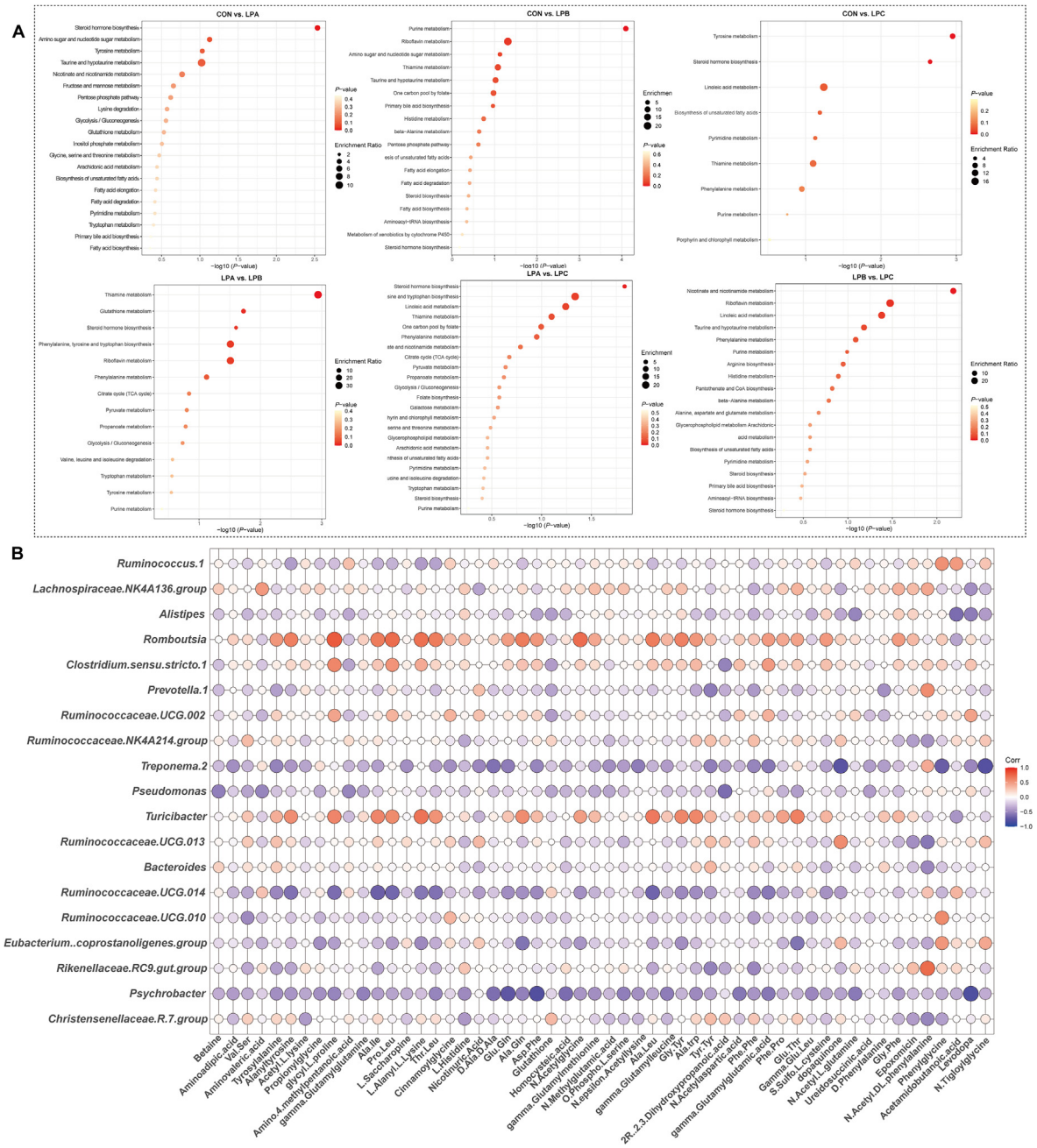

Fig. 4. Enrichment analysis of metabolic pathways of differential fecal metabolites across four treatments. (A) Kyoto Encyclopedia of Genes and Genomes (KEGG) pathway enrichment analysis performed using significantly different fecal metabolites based on pairwise comparisons (CON vs. LPA, CON vs. LPB, CON vs. LPC, LPA vs. LPB, LPA vs. LPC, and LPB vs. LPC). (B) Spearman's rank correlations between fecal microbiota (genus level) and microbial metabolites, predominantly comprising amino acids, peptides, and analogues, where blue circles represent negative correlations and red circles represent positive correlations. Treatments included CON (16.7% crude protein [CP] based on nutritional requirements), LPA, LPB, and LPC (CP decreased by approximately 10%, with SP proportions of 21.2%, 25.9%, and 29.4% of CP, respectively).

Ruminococcaceae family (especially *Ruminococcaceae UCG-005* at the genus level; Table S7). In contrast, these taxa showed negative correlations with NH_4^+—N and NO_2^-—N. On the other hand, NO_2^-—N, NH_4^+—N, and TN were identified as the top three factors impacting differential metabolite composition (Fig. 6B). Notably, Com7, Com64, Com75, and Com76 (primarily classified as AA and fatty acids; Table S7) were positively correlated with NO_2^-—N.

As shown in Fig. 6C, N metabolism phenotype indexes, except NO_2^-—N, showed strong positive correlations with urease and nitrate reductase activities as well as *gdh* gene abundance ($P < 0.01$). The concentration of the total SCFA was positively correlated with propionate but negatively correlated with butyrate ($P < 0.01$). Notably, the concentration of butyrate was negatively correlated with the abundance of gene *nirK* ($P < 0.05$). Furthermore, the abundance of *narG* gene was positively correlated with urease and nitrate reductase activities ($P < 0.05$), but negatively correlated with the concentration of propionate. From Mantel's test, urease and nitrate reductase activities were found to be correlated with fecal microbiota (Mantel's $P < 0.05$). Additionally, TN and urease activity were correlated with fecal differential metabolites in the AA classification (Mantel's $P < 0.05$); plasma ammonia concentration, total SCFA content, urease activity, and the abundance of *gdh*

Table 2
Blood routine examination and plasma biochemical indexes of sheep fed low-protein diets with different soluble protein (SP) levels.

Item	Treatments[1]				SEM	*P*-value
	CON	LPA	LPB	LPC		
Whole blood						
White blood cells, $\times10^9$/L	12.58	10.30	11.85	13.80	0.972	0.721
Red blood cells, $\times10^{12}$/L	10.81	11.13	11.25	11.56	0.181	0.576
Platelets, $\times10^9$/L	415.3	415.7	485.7	478.7	35.71	0.376
Hemoglobin, g/L	138.7	133.7	151.9	138.0	3.03	0.192
Plasma						
Total protein, g/L	73.08	65.47	68.13	58.70	2.362	0.139
Albumin, g/L	23.65	23.50	20.43	20.75	0.623	0.115
Globulin, g/L	49.43	41.97	47.70	37.95	2.337	0.262
Albumin/globulin	0.49	0.64	0.43	0.57	0.041	0.286
Creatinine, U/L	57.03^a	49.00^b	47.67^b	44.25^b	4.322	0.023
Ammonia, μmol/L	150.6^a	118.5^b	122.8^b	126.9^b	8.53	0.021
Urea nitrogen, mmol/L	13.38^a	9.67^b	7.20^b	8.35^b	0.826	0.001
Alkaline phosphatase, U/L	175.8	259.0	227.7	201.3	19.31	0.522
Lactate dehydrogenase, U/L	591.3	723.7	646.0	725.8	44.65	0.691
Cholesterol, mmol/L	1.63	1.69	1.54	1.67	0.085	0.947
Triglycerides, mmol/L	0.18	0.32	0.29	0.16	0.041	0.424
High-density lipoprotein, mmol/L	0.67	0.90	0.73	0.78	0.058	0.488
Low-density lipoprotein, mmol/L	0.59	0.55	0.52	0.61	0.033	0.837

SEM = standard error of the mean.
$^{a, b}$Within a row, means without a common superscript differed at $P < 0.05$.
[1] Treatments included CON (16.7% crude protein [CP] based on nutritional requirements), LPA, LPB, and LPC (CP decreased by approximately 10%, with SP proportions of 21.2%, 25.9%, and 29.4% of CP, respectively).

gene were associated with differential metabolites in the carbohydrate classification (Mantel's $P < 0.05$); plasma urea-N and ammonia, fecal TN, total SCFA, urease activity, and the abundance of *narG* gene were correlated with the plasma AA concentration (Mantel's $P < 0.05$).

4. Discussion

In a previous study, we examined the effects of reduced CP diets containing varying levels of SP levels on growth performance, nutrient digestibility, rumen microbiota and metabolites, as well as their potential associations with N metabolism (Zhang et al., 2021). In the present study, we attempted to focus on the impacts of these dietary treatments on intestinal N absorption, fecal microbiota, and metabolites, as well as their linkage with the N metabolism phenotype in feces, aiming to reveal the potential and mechanisms of nutrient manipulation, specifically N fraction, in the regulation of hindgut microbial fermentation, with the ultimate aim to mitigating reactive N emissions.

The counts of white blood cells and red blood cells in whole blood, along with total protein, globulin, and alkaline phosphatase in plasma, serve as indicators of animal humoral immunity and protein synthesis (Chen et al., 2015). In this study, physiological and biochemical parameters of blood in all sheep were in alignment with those of the previous studies (Peng et al., 2016; Sweeny et al., 2014). These parameters suggested that a modest reduction in dietary CP content (approximately 10%) did not adversely affect the metabolic and health status of the sheep. Notably, with the elevation of SP levels in low-protein diets, a declining trend in creatinine concentration was observed. This finding is consistent with previous reports (Xu et al., 2019), wherein creatinine concentration linearly decreased with an increase in dietary urea content (0, 10, 20, 30 g/kg) for fattening Hu sheep. The modulation of urea proportion was a pivotal factor in altering dietary SP levels in this study (Table S1), warranting further investigations to elucidate the relationship between SP levels and blood creatinine concentration. In addition, the reduction in dietary CP content led to decreased plasma ammonia and urea N concentrations, which was in concordance with our previous results on serum parameters (Zhang et al., 2021). It was noted that an increase in dietary SP (% CP) from 34.4% to 44.9% resulted in elevated ammonia and urea N concentrations (Wilson et al., 1998). However, no significant differences were observed in ammonia and urea N concentrations with the incremental rise in SP (% CP) in low-protein diets, potentially attributed to the lower addition of dietary urea. Further investigations are warranted to delineate this relationship.

The nutritional quality of protein entering the gut of ruminants, especially the small intestine, largely depends on the AA and peptide composition of microbial proteins within the forestomach (Merchen and Titgemeyer, 1992). It has been reported that microbial protein content was linearly correlated with dietary CP, suggesting that to some extent, increased dietary CP enhances the influx of AA and peptides into the intestine. Consequently, this may augment the delivery of AA and peptides across the intestinal epithelium into the bloodstream for utilization by target tissues (Ghorbani et al., 2011).

Our study revealed that lower plasma contents of AA, particularly essential AA, in the low-protein treatments compared with CON. Nevertheless, the transportation and absorption of AA and small peptides occur through distinct transporters in the intestinal epithelium (Broer, 2008). To assess the potential correlation between changes in the plasma AA concentration and the absorption process, we examined the mRNA expression levels of intestinal AA and peptide transporters. Notably, the duodenum, jejunum, and ileum of the LPA treatment exhibited decreased mRNA abundance of *SLC1A1*, *SLC7A2*, and *SLC7A8* compared with CON. *SLC1A1* is a Na^+-dependent glutamate transporter that can transfer glutamate and aspartate (Rao et al., 2021; Wang et al., 2022b). These two AA are involved in various metabolic processes, especially in intestinal integrity, protein synthesis, and energy metabolism (Lin et al., 2014; Pi et al., 2014). The concentrations of plasma glutamate and aspartate were upregulated in LPB and LPC compared to LPA, suggesting that enhanced intestinal nutrient utilization efficiency with an SP proportion of approximately 25% to 30%, simultaneously the evidence could also be found in the results of N absorption and N efficiency (Zhang et al., 2021). *SLC7A2* and *SLC7A8* were two important acidic AA transporters. The up-regulated expressions of *SLC7A2* and *SLC7A8* may contribute to heightened arginine

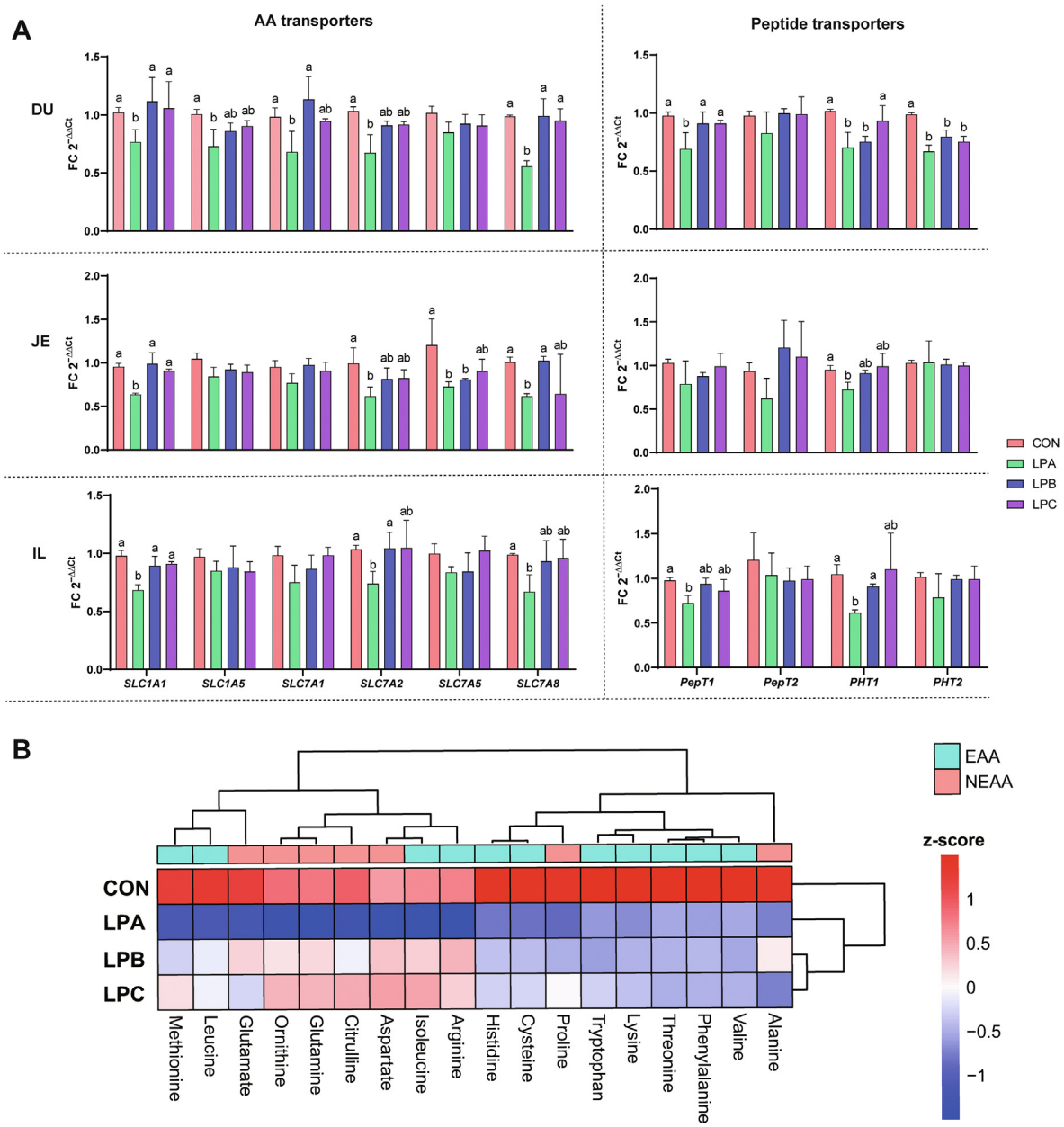

Fig. 5. Differential mRNA abundance of small intestinal amino acids (AA) and peptide transporters (A) and plasma AA concentrations (B) across four treatments. [a, b]Bars with different letters indicate a significant difference at $P < 0.05$. DU = duodenum, JE = jejunum, IL = ileum; EAA = essential amino acids, NEAA = non-essential amino acids. Treatments included CON (16.7% crude protein [CP] based on nutritional requirements), LPA, LPB, and LPC (CP decreased by approximately 10%, with soluble protein [SP] proportions of 21.2%, 25.9%, and 29.4% of CP, respectively).

absorption and protein synthesis, thereby improving the endogenous urea N cycle (Ding et al., 2019), which also explained the elevated plasma arginine content in LPB and LPC. Regarding peptide transporters, LPA exhibited decreased mRNA abundance of *PepT1* and *PHT1*, particularly *PHT1*. However, understanding how SP levels regulate intestinal peptide transport will require a systematic and thorough investigation.

Nutritional manipulation, involving adjustments and optimization of dietary CP levels, emerged as a highly effective strategy for mitigating fecal N emissions during the feeding stage, primarily through the modulation of the gut microbiome (Lynch et al., 2007). Numerous studies have consistently reported that a significant reduction in TN content in the ruminant feces and NH_3 emissions from manure management with decreased dietary CP levels (Lee et al., 2012; Sajeev et al., 2018). Furthermore, a recent study on weaned pigs (Lee et al., 2022) found a decrease in NH_4^+–N content in intestinal chyme as dietary CP content decreased. Our study corroborates these results, demonstrating a concurrent decline in TN and NH_4^+–N contents, as well as reduced urease activity and the abundance of *gdh* gene. This further substantiates the positive association between NH_4^+–N content and dietary N levels. Interestingly, no significant variations were observed with changing SP levels.

It is essential to highlight that urease activity in CON and LPA was notably higher, necessitating careful attention to manure management. Consistent with our previous study (Zhang et al., 2021), a higher urea N content in the urine of CON and LPA

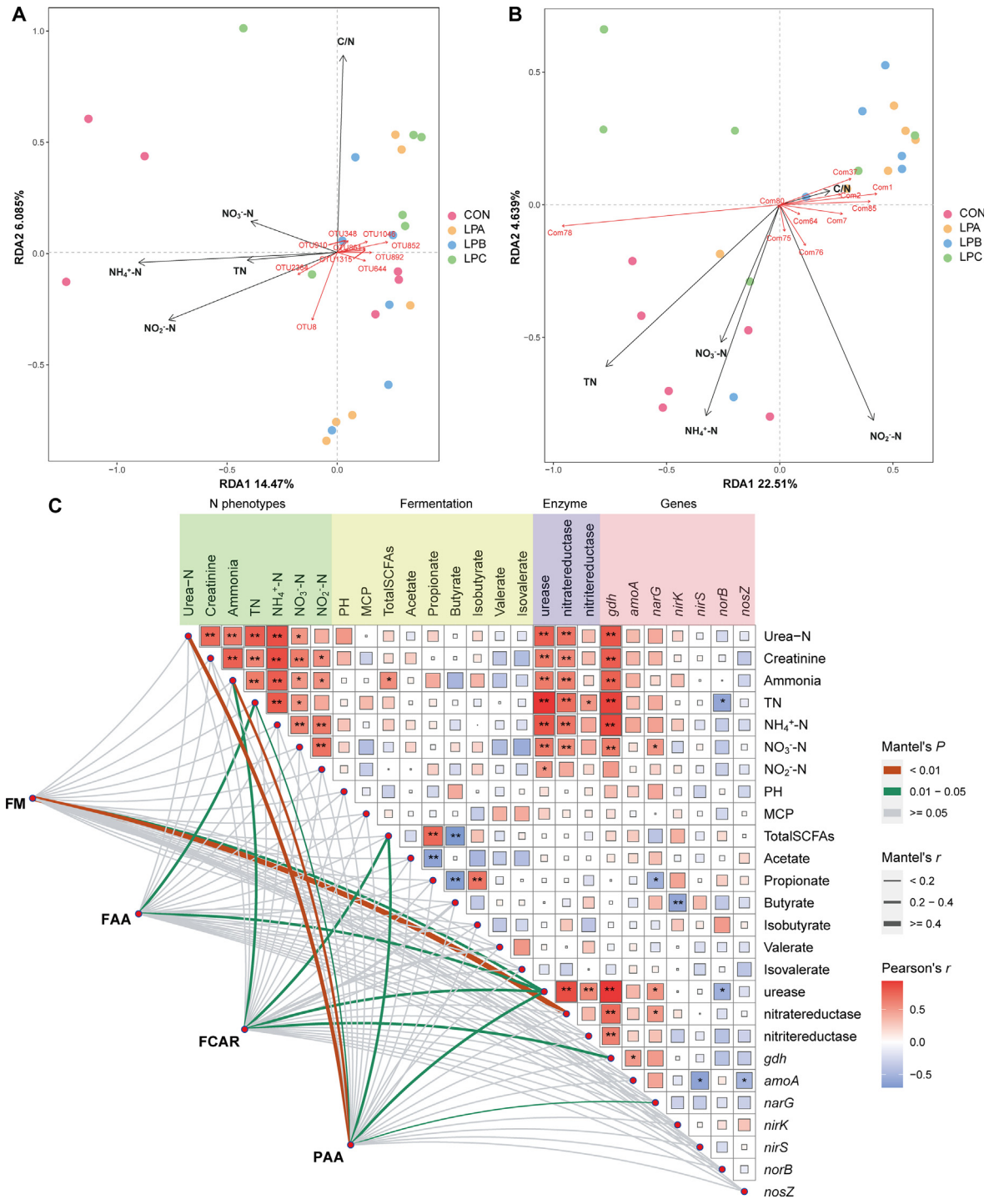

Fig. 6. Interactions of fecal microbiota, metabolites, plasma amino acids (AA) concentration and nitrogen (N) metabolism phenotypes. (A and B) Redundancy analysis (RDA) revealing the relationship between fecal N metabolism phenotypes and bacterial community at operational taxonomic unit (OTU) abundance (A) and the relationship between fecal metabolism phenotypes and differential metabolites (B). (C) Correlation analysis encompassing fecal metabolic N phenotype, fermentation indicators, enzyme activity, gene expression levels and fecal microbiota, and types of differential metabolites based on Mantel-test coefficient. * Means Pearson's $P < 0.05$ and ** means Pearson's $P < 0.01$. FM = fecal microbiota; FAA = fecal differential metabolites in amino acid classification; FCAR = fecal differential metabolites in carbohydrate classification; PAA = plasma AA concentration; TN = total nitrogen; NH_4^+−N = ammonia nitrogen; NO_3^-−N = nitrate nitrogen; NO_2^-−N = nitrite nitrogen; MCP = microbial crude protein; SCFA = short-chain fatty acids; *gdh* = glutamic acid dehydrogenase gene; *amoA* = ammonia monooxygenase gene subunit A; *narG* = nitrate reductase gene; *nirS*/*nirK* = nitrite reductase gene; *norB* = nitric oxide reductase gene; *nosZ* = nitrous oxide reductase gene.

groups emphasizes the imperative need to avoid mixing manure and urine. Such practices are crucial to prevent the substantial production of NH_3, as underscored by Powell et al. (2011).

The N cycle and associated gene abundance play a pivotal role in sustaining agricultural and livestock production (Wang et al., 2022a). Nitrate reductase and nitrite reductase are key

contributors to denitrification, transforming nitrate into N_2 or N_2O. Our findings align with those reported by Lycus et al. (2018), revealing a positive correlation between TN and nitrate reductase activity. Nitrate reductase facilitates N storage by enhancing organic N mineralization to NH_4^+–N, which is subsequently converted into stable N compounds by nitrate reductase, contributing to its storage in manure products (Chen et al., 2019).

Notably, LPB demonstrated a decrease in nitrate reductase activity compared to CON, accompanied by down-regulation in NO_2^-–N content and *narG* gene abundance. The *narG* gene encodes a membrane-bound nitrate reductase catalyzing nitrate reduction to nitrite under anaerobic conditions (Ramírez-Fernández et al., 2021). Furthermore, LPB and LPC exhibited reduced abundance of the *nirS* gene, with no significant difference observed in the *nirK* gene. According to Heylen et al. (2006), the nitrite reductase encoded by the *nirS* gene has a higher affinity for electrons in denitrification compared with the *nirK* gene, suggesting a potential reduction in intestinal denitrifying bacteria in LPB and LPC.

Additionally, the abundance of the *norB* gene decreased in LPB and LPC, possibly contributing to decreased intestinal N_2O emissions. These findings underscore the need for future systematic studies to comprehensively investigate the intricate relationships within the microbial community impacting N cycling.

Hindgut microbiota fermentation primarily yielded SCFA, such as acetate, propionate, and butyrate. Contrary to general expectations of increased long-chain fatty acids (i.e. valerate) during the fermentation of N-containing compounds (Le et al., 2009; Smith and Macfarlane, 1998), our study revealed no significant variation in valerate proportions. This suggests that intestinal fermentation is still dominated by carbohydrates. Notably, diminished dietary protein levels have been reported to reduce the concentrations of the total SCFA and propionate in the hindgut of the Göttingen Mini-pig (Xu et al., 2020), which is consistent with the findings in our study.

Fecal microbiota analysis indicated a reduction in the abundance of *Psychrobacter* in feces with low-protein diets, correlating with decreased organic matter degradation and carbohydrate fermentation (Kämpfer et al., 2002; Ma et al., 2020). Additionally, the distinctive fecal metabolite profile of the CON group primarily is concentrated in AA, nucleotide sugar metabolism, and unsaturated fat acid biosynthesis. This emphasizes the impact of dietary composition on hindgut microbiota and associated metabolic pathways, providing insights into the modulation of microbial activity through protein levels in the diet.

When the SP level was adjusted to 21.2% of CP in low-protein diets, a notable decrease in the SCFA concentration and the proportion of propionate was observed compared with SP levels at 25.9% and 29.4% of CP. Conversely, the proportion of butyrate increased, reflecting the available fermented nutrients in the hindgut, the balance between C and N degradation, and microbial diversity (Perea et al., 2017). Remarkably, *Desulfovibrio*, which is characterized by the use of lactate, pyruvate, ethanol or some fatty acids as carbon sources, significantly enriched in LPA, thereby promoting sulfate reduction to hydrogen sulfide and increasing butyrate production (Chen et al., 2021; Devereux et al., 1990).

Additionally, an increase in intestinal butyrate production in goats fed with high rumen undegradable protein is associated with the enrichment of gut *Eubacterium* members that contribute to butyrate production (Wu et al., 2022). In line with our previous results on rumen microbiome, Prevotellaceae and *Prevotella* in feces are enriched in diets with an SP proportion of approximately 25% to 30% of CP, playing a vital role in intestinal SCFA synthesis, particularly in utilizing arabinoxylan and oligofructose for propionate production (Gálvez et al., 2020; Kovatcheva-Datchary et al., 2015).

Moreover, adjusting SP to 25.9% and 29.4% of CP in low-protein diets led to an increase in Patescibacteria abundance, actively participating in denitrification and reducing the accumulation of NO_2^-, NO, and N_2O. Patescibacteria has shown an ability in the reduction of NO_2^-–N by involving in denitrification (Yang et al., 2022b). Patescibacteria also mitigates energy loss caused by environmental changes in ungulates (Wang et al., 2022c), thereby improving nutrient utilization efficiency. Furthermore, the abundance of *Candidatus Saccharimonas*, *Ruminiclostridium 9*, and *Lachnospiraceae UCG-004* was improved. It is shown that the enrichment of these genera in feces is beneficial for improving metabolic syndrome and maintaining intestinal homeostasis (Xu et al., 2022; Yang et al., 2022a).

Pathway enrichment analysis showed that with the increase of SP levels in low-protein diets, pyruvate and propionate metabolism increased, which further provided evidence to support the conclusions we have drawn. In addition, thiamine metabolism was enhanced in LPB and LPC compared with LPA, highlighting the importance of thiamine as a coenzyme in the catabolism of sugar and AA, and its pivotal role in carbohydrate energy release. Thiamine deficiency reduces the activity of pyruvate dehydrogenase, leading to lactate accumulation. Therefore, thiamine therapy is considered a potential strategy for improving metabolic pathways (Fujii et al., 2020; Nozaki et al., 2009). Recent studies have suggested that thiamine supplementation may regulate energy metabolism disorders in lipopolysaccharide-induced rumen epithelial cells (Ma et al., 2022), indicating the potential detriment of lower SP levels to energy and N metabolism homeostasis (Henning et al., 1993).

In this study, the abundance of fecal microbiota demonstrated a close association with urease and nitrate reductase activities. Urease, in particular, exhibited links with distinct AA and carbohydrate metabolites, influencing the transformation of N phenotype forms in feces, including NH_4^+–N and NO_2^-–N contents. RDA analysis highlighted these enzymatic activities as primary drivers of fecal microbiota and metabolites. Therefore, effective reduction of ruminant N excretion requires not only adjustments to nutrition manipulation strategies but also the consideration of the microbial community structure and functional characteristics across different ecological niches throughout the entire digestive tract. Concurrently, ecological strategies are required to maximize the efficacy of N emission reduction in manure management.

5. Conclusions

Decreasing dietary CP content by approximately 10% emerges as a promising strategy to mitigate N emissions from the source. Notably, fine-tuning the dietary SP levels to 25% to 30% of CP in low-protein diets demonstrated an amplifying effect. This adjustment not only contributed to a decline in fecal urease activity but also led to a reduction in NH_4^+–N and NO_2^-–N contents, facilitated by the enrichment of the *Prevotella* genus. The observed up-regulation in mRNA abundance of intestinal AA and peptide transporters, coupled with elevated plasma AA concentrations, underscores a significant enhancement in N efficiency. This nuanced dietary intervention, therefore, holds promise for optimizing N utilization in livestock. Furthermore, our findings highlight the intricate relationship between dietary SP level and the urea N cycle. The variations in plasma urea cycle-related AA with SP levels underscore the need for future comprehensive investigations into the systemic responses of the urea N cycle to dietary SP manipulations.

Such endeavors are essential for advancing our understanding and refining strategies for sustainable and efficient N management in animal production systems.

Author contributions

Zhenbin Zhang: Conceptualization; Formal analysis; Investigation; Data curation; Software; Visualization; Writing - original draft; Writing - review & editing. **Yiquan Sun:** Formal analysis; Investigation; Data curation; Software. **Xinhuang Zhong**, **Jun Zhu**, **Sihan Yang, Yalan Gu** and **Xiang Yu:** Investigation, Data curation. **Yue Lu** and **Zhiqi Lu:** Investigation. **Xuezhao Sun:** Writing-review & editing. **Mengzhi Wang:** Conceptualization; Formal analysis; Investigation; Writing-review & editing; Funding acquisition; Project administration; Resources; Supervision.

Data availability statement

The sequencing datasets presented in this study can be found in online repositories: NCBI SRA BioProject (accession no: PRJNA780247; BioSample accession: SAMN39943842).

Declaration of competing interest

We declare that we have no financial and personal relationships with other people or organizations that can inappropriately influence our work, and there is no professional or other personal interest of any nature or kind in any product, service and/or company that could be construed as influencing the content of this paper.

Acknowledgements

This study was financially supported by Bintuan Science and Technology Program (2023AB078); Bintuan Agricultural Innovation Project (NCG202232); China Scholarship Council (NO. 20220 8320271), Postgraduate Research & Practice Innovation Program of Jiangsu Province (KYCX22_3532, SJCX23_1991) and the Priority Academic Program Development of Jiangsu Higher Education Institutions (PAPD), China.

Appendix Supplementary data

Supplementary data to this article can be found online at https://doi.org/10.1016/j.aninu.2024.04.003.

References

AOAC. Official methods of analysis. 18th ed. Gaithersburg, MD, USA: AOAC International; 2005.
Bai Z, Ma L, Jin S, Ma W, Velthof GL, Oenema O, Liu L, Chadwick D, Zhang F. Nitrogen, phosphorus, and potassium flows through the manure management chain in China. Environ Sci Technol 2016;50:13409–18.
Barnett D, Arts I, Penders J. microViz: an R package for microbiome data visualization and statistics. J Open Source Softw 2021;6:3201.
Broer S. Amino acid transport across mammalian intestinal and renal epithelia. Physiol Rev 2008;88:249–86.
Chambers JM. Software for data analysis: programming with R, vol. 2. Springer; 2008.
Chappidi S, Villa EC, Cantarel BL. Using Mothur to determine bacterial community composition and structure in 16S ribosomal RNA datasets. Curr Protoc Bioinformatics 2019;67:e83.
Chen GJ, Song SD, Wang BX, Zhang ZF, Peng ZL, Guo CH, Zhong JC, Wang Y. Effects of forage:concentrate ratio on growth performance, ruminal fermentation and blood metabolites in housing-feeding yaks. Asian-Australas J Anim Sci 2015;28:1736–41.
Chen M, Wang C, Wang B, Bai X, Gao H, Huang Y. Enzymatic mechanism of organic nitrogen conversion and ammonia formation during vegetable waste composting using two amendments. Waste Manag 2019;95:306–15.
Chen S, Zhou Y, Chen Y, Gu J. fastp: an ultra-fast all-in-one FASTQ preprocessor. Bioinformatics 2018;34:i884–90.
Chen YR, Jing QL, Chen FL, Zheng H, Chen LD, Yang ZC. Desulfovibrio is not always associated with adverse health effects in the Guangdong Gut Microbiome Project. PeerJ 2021;9:e12033.
Cheng L, Zhang X, Reis S, Ren C, Xu J, Gu B. A 12% switch from monogastric to ruminant livestock production can reduce emissions and boost crop production for 525 million people. Nat Food 2022;3:1040–51.
Conway JR, Lex A, Gehlenborg N. UpSetR: an R package for the visualization of intersecting sets and their properties. Bioinformatics 2017;33:2938–40.
Devereux R, He SH, Doyle CL, Orkland S, Stahl DA, LeGall J, Whitman WB. Diversity and origin of Desulfovibrio species: phylogenetic definition of a family. J Bacteriol 1990;172:3609–19.
Ding L, Shen Y, Wang Y, Zhou G, Zhang X, Wang M, Loor JJ, Chen L, Zhang J. Jugular arginine supplementation increases lactation performance and nitrogen utilization efficiency in lactating dairy cows. J Anim Sci Biotechnol 2019;10:3.
Edgar RC. UPARSE: highly accurate OTU sequences from microbial amplicon reads. Nat. Methods 2013;10:996–8.
Fahy E, Sud M, Cotter D, Subramaniam S. LIPID MAPS online tools for lipid research. Nucleic Acids Res 2007;35:W606–12.
FAOSTAT. Food and Agriculture Organization of the United Nations. 2021.
Fujii T, Deane AM, Nair P. Metabolic support in sepsis: corticosteroids and vitamins: the why, the when, the how. Curr Opin Crit Care 2020;26:363–8.
Gálvez EJC, Iljazovic A, Amend L, Lesker TR, Renault T, Thiemann S, Hao L, Roy U, Gronow A, Charpentier E, et al. Distinct polysaccharide utilization determines interspecies competition between intestinal Prevotella spp. Cell Host Microbe 2020;28:838–852.e6.
Geng RQ, Chang H, Yang ZP, Sun W, Wang LP, Lu SX, Tsunoda K, Ren ZJ. Study on origin and phylogeny status of Hu sheep. Asian-Australas J Anim Sci 2003;16:743–7.
Ghorbani B, Ghoorchi T, Amanlou H, Zerehdaran S. Effects of using monensin and different levels of crude protein on milk production, blood metabolites and digestion of dairy cows. Asian-Australas J Anim Sci 2011;24:65–72.
Harris AR, Pickering AJ, Harris M, Doza S, Islam MS, Unicomb L, Luby S, Davis J, Boehm AB. Ruminants contribute fecal contamination to the urban household environment in Dhaka, Bangladesh. Environ Sci Technol 2016;50:4642–9.
Henning PH, Steyn DG, Meissner HH. Effect of synchronization of energy and nitrogen supply on ruminal characteristics and microbial growth1. J Anim Sci 1993;71:2516–28.
Heylen K, Gevers D, Vanparys B, Wittebolle L, Geets J, Boon N, De Vos P. The incidence of nirS and nirK and their genetic heterogeneity in cultivated denitrifiers. Environ Microbiol 2006;8:2012–21.
Hu L, Chen Y, Cortes IM, Coleman DN, Dai H, Liang Y, Parys C, Fernandez C, Wang M, Loor JJ. Supply of methionine and arginine alters phosphorylation of mechanistic target of rapamycin (mTOR), circadian clock proteins, and α-s1-casein abundance in bovine mammary epithelial cells. Food Funct 2020;11:883–94.
Huang C, Li ZL, Chen F, Liu Q, Zhao YK, Zhou JZ, Wang AJ. Microbial community structure and function in response to the shift of sulfide/nitrate loading ratio during the denitrifying sulfide removal process. Bioresour Technol 2015;197:227–34.
Kämpfer P, Albrecht A, Buczolits S, Busse HJ. Psychrobacter faecalis sp. nov., a new species from a bioaerosol originating from pigeon faeces. Syst Appl Microbiol 2002;25:31–6.
Kanehisa M, Goto S. KEGG: Kyoto Encyclopedia of Genes and Genomes. Nucleic Acids Res 2000;28:27–30.
Koontz L. Chapter one - TCA precipitation. In: Lorsch J, editor. Methods Enzymol, vol. 541. Academic Press; 2014. p. 3–10.
Kovatcheva-Datchary P, Nilsson A, Akrami R, Lee YS, De Vadder F, Arora T, Hallen A, Martens E, Bjorck I, Backhed F. Dietary fiber-induced improvement in glucose metabolism is associated with increased abundance of Prevotella. Cell Metab 2015;22:971–82.
Le PD, Aarnink AJA, Jongbloed AW. Odour and ammonia emission from pig manure as affected by dietary crude protein level. Livest Sci 2009;121:267–74.
Lee C, Hristov AN, Dell CJ, Feyereisen GW, Kaye J, Beegle D. Effect of dietary protein concentration on ammonia and greenhouse gas emitting potential of dairy manure. J Dairy Sci 2012;95:1930–41.
Lee J, Htoo JK, Kluenemann M, González-Vega C, Nyachoti M. PSX-A-4 effects of dietary protein content and crystalline amino acid supplementation patterns on intestinal bacteria and their metabolites in weaned pigs raised under different sanitary conditions. J Anim Sci 2022;100:279–80.
Licitra G, Hernandez TM, Van Soest PJ. Standardization of procedures for nitrogen fractionation of ruminant feeds. Anim Feed Sci Technol 1996;57:347–58.
Lin M, Zhang B, Yu C, Li J, Zhang L, Sun H, Gao F, Zhou G. L-glutamate supplementation improves small intestinal architecture and enhances the expressions of jejunal mucosa amino acid receptors and transporters in weaning piglets. PLoS One 2014;9:e111950.
Livak KJ, Schmittgen TD. Analysis of relative gene expression data using real-time quantitative PCR and the 2(-Delta Delta C(T)) Method. Methods 2001;25:402–8.
Lycus P, Soriano-Laguna MJ, Kjos M, Richardson DJ, Gates AJ, Milligan DA, Frostegard A, Bergaust L, Bakken LR. A bet-hedging strategy for denitrifying bacteria curtails their release of N2O. Proc Natl Acad Sci U S A 2018;115:11820–5.
Lynch MB, Sweeney T, Callan BFJJ, O'Doherty JV. The effect of high and low dietary crude protein and inulin supplementation on nutrient digestibility, nitrogen excretion, intestinal microflora and manure ammonia emissions from finisher pigs. Animal 2007;1:1112–21.

Ma J, Zhu Y, Wang Z, Yu X, Hu R, Wang X, Cao G, Zou H, Shah AM, Peng Q, et al. Comparing the bacterial community in the gastrointestinal tracts between growth-retarded and normal yaks on the Qinghai–Tibetan Plateau. Front Microbiol 2020;11:600516.
Ma Y, Elmhadi M, Wang C, Li Z, Zhang H, He B, Zhao X, Zhang Z, Wang H. Thiamine supplementation alleviates lipopolysaccharide-triggered adaptive inflammatory response and modulates energy state via suppression of NFκB/p38 MAPK/AMPK signaling in rumen epithelial cells of goats. Antioxidants 2022;11:2048.
Magoc T, Salzberg SL. FLASH: fast length adjustment of short reads to improve genome assemblies. Bioinformatics 2011;27:2957–63.
Merchen NR, Titgemeyer EC. Manipulation of amino acid supply to the growing ruminant. J Anim Sci 1992;70:3238–47.
Norusis M. SPSS 16.0 statistical procedures companion. Prentice Hall Press; 2008.
Noyes H. Accurate determination of soil nitrates by phenol disulfonic acid method. Ind Eng Chem 1919;11:213–8.
Nozaki S, Mizuma H, Tanaka M, Jin G, Tahara T, Mizuno K, Yamato M, Okuyama K, Eguchi A, Akimoto K, et al. Thiamine tetrahydrofurfuryl disulfide improves energy metabolism and physical performance during physical-fatigue loading in rats. Nutr Res 2009;29:867–72.
NRC (National Research Council). Nutrient requirements of small ruminants: sheep, goats, cervids, and new world camelids. Washington (DC): The National Academy Press; 2007.
Oksanen J, Kindt R, Legendre P, O'Hara B, Stevens MHH, Oksanen MJ, Suggests M. The vegan package. Community ecology package10; 2007. p. 719.
Pang Z, Chong J, Zhou G, de Lima Morais DA, Chang L, Barrette M, Gauthier C, Jacques P-É, Li S, Xia J. MetaboAnalyst 5.0: narrowing the gap between raw spectra and functional insights. Nucleic Acids Res 2021;49:W388–96.
Peng K, Shirley DC, Xu Z, Huang Q, McAllister TA, Chaves AV, Acharya S, Liu C, Wang S, Wang Y. Effect of purple prairie clover (Dalea purpurea Vent.) hay and its condensed tannins on growth performance, wool growth, nutrient digestibility, blood metabolites and ruminal fermentation in lambs fed total mixed rations. Anim Feed Sci Technol 2016;222:100–10.
Perea K, Perz K, Olivo SK, Williams A, Lachman M, Ishaq SL, Thomson J, Yeoman CJ. Feed efficiency phenotypes in lambs involve changes in ruminal, colonic, and small-intestine-located microbiota1. J Anim Sci 2017;95:2585–92.
Pi D, Liu Y, Shi H, Li S, Odle J, Lin X, Zhu H, Chen F, Hou Y, Leng W. Dietary supplementation of aspartate enhances intestinal integrity and energy status in weanling piglets after lipopolysaccharide challenge. J Nutr Biochem 2014;25:456–62.
Powell JM, Aguerre MJ, Wattiaux MA. Tannin extracts abate ammonia emissions from simulated dairy barn floors. J Environ Qual 2011;40:907–14.
Ramírez-Fernández L, Orellana LH, Johnston ER, Konstantinidis KT, Orlando J. Diversity of microbial communities and genes involved in nitrous oxide emissions in Antarctic soils impacted by marine animals as revealed by metagenomics and 100 metagenome-assembled genomes. Sci Total Environ 2021;788:147693.
Rao Y, Kuang Z, Li C, Guo S, Xu Y, Zhao D, Hu Y, Song B, Jiang Z, Ge Z, et al. Gut Akkermansia muciniphila ameliorates metabolic dysfunction-associated fatty liver disease by regulating the metabolism of L-aspartate via gut-liver axis. Gut Microbes 2021;13:1–19.
Revelle WR. psych: procedures for personality and psychological research. Evanston, Illinois, USA: Northwestern University; 2017. Version = 1.7.8.
Rognes T, Flouri T, Nichols B, Quince C, Mahé F. VSEARCH: a versatile open source tool for metagenomics. PeerJ 2016;4.
Sabharwal S. Determination of nitrite ion by differential-pulse polarography using N-(1-naphthyl) ethylenediamine. Analyst 1990;115:1305–7.
Sajeev EPM, Amon B, Ammon C, Zollitsch W, Winiwarter W. Evaluating the potential of dietary crude protein manipulation in reducing ammonia emissions from cattle and pig manure: a meta-analysis. Nutr Cycl Agroecosyst 2018;110:161–75.
Smith EA, Macfarlane GT. Enumeration of amino acid fermenting bacteria in the human large intestine: effects of pH and starch on peptide metabolism and dissimilation of amino acids. FEMS Microbiol Ecol 1998;25:355–68.
Sweeny JPA, Surridge V, Humphry PS, Pugh H, Mamo K. RETRACTED: benefits of different urea supplementation methods on the production performances of Merino sheep. Vet J 2014;200:398–403.
Tan P, Liu H, Zhao J, Gu X, Wei X, Zhang X, Ma N, Johnston LJ, Bai Y, Zhang W, et al. Amino acids metabolism by rumen microorganisms: nutrition and ecology strategies to reduce nitrogen emissions from the inside to the outside. Sci Total Environ 2021;800:149596.
Terrlink T, van Leeuwen PA, Houdijk A. Plasma amino acids determined by liquid chromatography within 17 minutes. Clin Chem 1994;40:245–9.
Tilman D, Clark M. Global diets link environmental sustainability and human health. Nature 2014;515.
Uwizeye A, de Boer IJM, Opio CI, Schulte RPO, Falcucci A, Tempio G, Teillard F, Casu F, Rulli M, Galloway JN, et al. Nitrogen emissions along global livestock supply chains. Nat Food 2020;1:437–46.
van der Weerden TJ, Noble AN, Luo J, de Klein CAM, Saggar S, Giltrap D, Gibbs J, Rys G. Meta-analysis of New Zealand's nitrous oxide emission factors for ruminant excreta supports disaggregation based on excreta form, livestock type and slope class. Sci Total Environ 2020;732:139235.
Wang F, Fang Y, Wang L, Xiang H, Chen G, Chang X, Liu D, He X, Zhong R. Effects of residual monensin in livestock manure on nitrogen transformation and microbial community during "crop straw feeding-substrate fermentation-mushroom cultivation" recycling system. Waste Manag 2022a;149:333–44.
Wang X, Chen Z, Xu J, Tang S, An N, Jiang L, Zhang Y, Zhang S, Zhang Q, Shen Y, et al. SLC1A1-mediated cellular and mitochondrial influx of R-2-hydroxyglutarate in vascular endothelial cells promotes tumor angiogenesis in IDH1-mutant solid tumors. Cell Res 2022b;32:638–58.
Wang XB, Wu XY, Shang YQ, Gao Y, Li Y, Wei QG, Dong YH, Mei XS, Zhou SY, Sun GL, et al. High-altitude drives the convergent evolution of alpha diversity and indicator microbiota in the gut microbiomes of ungulates. Front Microbiol 2022c;13:953234.
Wickham H. ggplot2. WIREs Comp Stat 2011;3:180–5.
Wickham H, Averick M, Bryan J, Chang W, McGowan L, François R, Grolemund G, Hayes A, Henry L, Hester J, et al. Package tidyverse. J Open Source Softw 2017;43:1686.
Wilson RC, Overton TR, Clark JH. Effects of Yucca shidigera extract and soluble protein on performance of cows and concentrations of urea nitrogen in plasma and milk. J Dairy Sci 1998;81:1022–7.
Wishart DS, Tzur D, Knox C, Eisner R, Guo AC, Young N, Cheng D, Jewell K, Arndt D, Sawhney S, et al. HMDB: the human metabolome database. Nucleic Acids Res 2007;35:D521–6.
Wu J, Zhang X, Wang M, Zhou C, Jiao J, Tan Z. Enhancing metabolic efficiency through optimizing metabolizable protein profile in a time progressive manner with weaned goats as a model: involvement of gut microbiota. Microbiol Spectr 2022;10:e02545-21.
Xu SS, Wang N, Huang L, Zhang XL, Feng ST, Liu SS, Wang Y, Liu ZG, Wang BY, Wu TW, et al. Changes in the mucosa-associated microbiome and transcriptome across gut segments are associated with obesity in a metabolic syndrome porcine model. Microbiol Spectr 2022;10.
Xu Y, Curtasu MV, Bendiks Z, Marco ML, Nørskov N P, Knudsen KEB, Hedemann MS, Lærke HN. Effects of dietary fibre and protein content on intestinal fibre degradation, short-chain fatty acid and microbiota composition in a high-fat fructose-rich diet induced obese Göttingen Minipig model. Food Funct 2020;11:10758–73.
Xu Y, Li Z, Moraes LE, Shen J, Yu Z, Zhu W. Effects of incremental urea supplementation on rumen fermentation, nutrient digestion, plasma metabolites, and growth performance in fattening lambs. Animals 2019;9:652.
Yang C, Huang S, Lin Z, Chen H, Xu C, Lin Y, Sun H, Huang F, Lin D, Guo F. Polysaccharides from Enteromorpha prolifera alleviate hypercholesterolemia via modulating the gut microbiota and bile acid metabolism. Food Funct 2022a;13:12194–207.
Yang X, Yuan JL, Guo WJ, Tang XH, Zhang SY. The enzymes-based intermediary model explains the influence mechanism of different aeration strategies on nitrogen removal in a sequencing batch biofilm reactor treating simulated aquaculture wastewater. J Clean Prod 2022b;356.
Yue GH. Reproductive characteristics of Chinese Hu sheep. Anim Reprod Sci 1996;44:223–30.
Yuen SH, Pollard AG. Determination of nitrogen in agricultural materials by the nessler reagent. II.—Micro-determinations in plant tissue and in soil extracts. J Sci Food Agric 1954;5:364–9.
Zhang Z, Shahzad K, Shen S, Dai R, Lu Y, Lu Z, Li C, Chen Y, Qi R, Gao P, et al. Altering dietary soluble protein levels with decreasing crude protein may be a potential strategy to improve nitrogen efficiency in Hu sheep based on rumen microbiome and metabolomics. Front Nutr 2021;8:815358.
Zhang Z, Wei W, Yang S, Huang Z, Li C, Yu X, Qi R, Liu W, Loor JJ, Wang M, et al. Regulation of dietary protein solubility improves ruminal nitrogen metabolism in vitro: role of bacteria–protozoa interactions. Nutrients 2022;14:2972.